∗-Aware Charging of Lithium-ion Battery Cells

Liang He, Eugene Kim, and Kang G. Shin
The University of Michigan, Ann Arbor, MI, USA
{lianghe, kimsun, kgshin}@umich.edu

ABSTRACT

Lithium-ion cells are widely used in various platforms, such as electric vehicles (EVs) and mobile devices. Complete and fast charging of cells has always been the goal for sustainable system operation. However, fast charging is not always the best solution, especially in view of a new finding that cells need to rest/relax after being charged with high current to avoid accelerated capacity fading. Fast charging for its typical *Charge-and-Go* scenario does not allow this needed relaxation. In this paper, we propose ∗-Aware, a novel charging algorithm which maximizes the charged capacity within the user-specified available charging time (i.e., user-awareness) while ensuring enough relaxation (i.e., cell-awareness). We motivate and evaluate ∗-Aware via extensive measurements over 10 months. ∗-Aware is shown to improve the charged capacity by 6.9–50.5% over other charging algorithms that also ensure relaxation, and by almost 3x in some extreme cases. Furthermore, ∗-Aware slows down the capacity fading by 49.55% when compared to fast charging.

Categories and Subject Descriptors

C.3 [**Process control systems**]: Miscellaneous

General Terms

Design

Keywords

Battery charging, relaxation, CCCV charge, capacity fading

1. INTRODUCTION

The excellent cycle life and high power density of Lithium-ion cells [1] have made them widely adopted in Cyber-Physical Systems (CPSes) such as electric vehicles [2, 3], and mobile devices such as tablets and smartphones. For example, the battery pack of Tesla S 85D is built with 7,104 Lithium-ion cells [4]. Fast charging of battery cells has always been the goal to improve the sustainable system operation [5–7]. Various fast charging technologies have been designed and implemented, significantly reducing the time to charge the cells [8–12].

However, fast charging is not always the best solution for the following reasons. First, even the state-of-the-art fast charging technologies still take hours to fully charge cells. For example, it takes ≈ 100 minutes to fully charge a QC 2.0 supported Galaxy S6 Edge smartphone, although about 75% of the charging can be completed in 50 minutes. This large charging time may be unacceptable when the user has only a limited time to charge the battery. Second, fast charging is not necessary in many cases because most users are likely to charge the battery in the night [5, 13], which does not have to be fast. Moreover, the user may not need to fully charge the battery during the day time; the capacity enough for day-time usage could suffice. Last but not the least, fast charging accelerates the capacity fading of cells [14], which becomes even more pronounced because allowing cells to rest/relax for a certain time after charging with high current slows down their capacity fading. This new observation complements the conventional wisdom that relaxation-after-discharge improves the cycling performance of cells [15]. Fast charging, with its typical *Charge-and-Go* scenario, does not allow such relaxation. Accelerated capacity fading shortens the life of cells, increasing the system operation cost, e.g., the EV battery pack costs $30–40k and its warranty only covers limited capacity fading [16].

In this paper, we address the cell charging problem from a new perspective and aim to *maximize the charged capacity within the user-specified available charging time while ensuring enough time for cell relaxation*. Specifically, we propose ∗-Aware, a charging algorithm with both user- and cell-awareness and validate its design and performance with 10+-month measurements. ∗-Aware offers an attractive alternative when fast charging is not absolutely required, extending the battery lifetime.

The challenges in ∗-Aware arise from two aspects. First, the objective of maximizing the charged capacity and meeting the relaxation requirement generates an inherent conflict. ∗-Aware mitigates this conflict based on the finding that the constant-voltage charge (CV-Chg) — the second phase in the classic CCCV method [17] after the constant-current charge (CC-Chg) — also serves as relaxation and thus allows more charging capacity. However, exploiting CV-Chg as relaxation poses another challenge because with CCCV, charging less capacity does not necessarily lead to less required charging time, making the trade-off between

978-1-5090-1772-0/16/$31.00 ©2016 IEEE

the two non-trivial choices. ∗-AWARE addresses this by separating the control over CC-Chg from that over CV-Chg to identify the optimal charging profile in a reduced search space.

This paper makes the following contributions.

- We demonstrate that fast charging is not always the best and cells need relaxation after charging them with high currents in order to avoid accelerated capacity fading (Sec. 3).
- We discover that the completed CV-Chg of CCCV serves as relaxation (Sec. 4).
- We propose ∗-AWARE for charging Lithium-ion cells while considering both the user-specified available charge time and the required relaxation of cells, providing an alternative when fast charging is not required and gaining extended battery lifetime (Sec. 5).
- We evaluate ∗-AWARE both experimentally and via trace-driven emulations, showing that ∗-AWARE improves the charged capacity by 6.9–50.5% (up to 3x in some extreme cases), and slows down the capacity fading by 49.55% (Sec. 6).

The paper is organized as follows. Sec. 2 introduces the background on cell charging. Sec. 3 motivates the charging problem addressed in this paper. The exploration on CV-Chg as relaxation is described in Sec. 4. ∗-AWARE is detailed in Sec. 5 and evaluated in Secs. 6. Sec. 7 reviews the related literature. The paper concludes in Sec. 8.

2. BACKGROUND

Below we introduce the necessary background on the charging of battery cells.

• **C-Rate of Cells.** The performance of Lithium-ion cells hinges critically on how fast they are charged/discharged [18–20], which in turn has to be defined with regard to their rated capacity; for example, a 200mA charging current would be considered large for cells with 200mAh rated capacity but small for 2,600mAh cells. The charging (and discharging) currents of cells are often expressed in C-rate to capture this dependency. Specifically, taking cell discharging as an example, a 1C rate is the current drains the cell completely in 1 hour, i.e., 200mA for 200mAh cells and 2,600mA for 2,600mAh cells.

• **Open Circuit and Terminal Voltages.** The *open circuit voltage* (OCV) of a cell is the voltage between its terminals without load, which becomes the *terminal voltage* of the cell when the load is connected. In other words, OCV is an inherent property of the cell and the terminal voltage is what we can measure. The relationship between OCV and the terminal voltage can be described by the cell circuit model shown in Fig. 1:

$$V_{\text{terminal}} = OCV \pm I \cdot r, \tag{1}$$

where the cell is charged/discharged with current I, and r is the internal resistance of the cell. We use the term *voltage* for short when referring to the *terminal voltage* in the rest of this paper.

3. FAST CHARGE IS NOT ALWAYS BEST!

Fast charging has always been the goal to improve the sustainable system operation. However, we argue that fast charging is not always the best based on the following three observations.

• **Faster ≠ Fast Enough.** The first observation is that even the state-of-the-art fast charging technologies still take hours to fully charge the cells. Fig. 2 plots the charging processes of 5 mobile devices with their respective chargers: a Nexus S (2010), a Note 8.0 (2013), a Xperia Z (2013), a Galaxy 5S (2014), and a Galaxy S6 Edge (2015). The time to fully charge the devices has been shortened, e.g., from 3–4 hours for Nexus S to ≈2 hours for Galaxy S5. However, even the QC 2.0 supported Galaxy S6 Edge still takes ≈100 minutes to be fully charged.[1] Let us take EV charging as another example, which emphasizes more on fast charging due to the *range anxiety* [22]. Table 1 compares the three commonly seen EV charging technologies: Level 1–3 charging. Again, even the fastest Level-3 charging requires 30min to charge the batteries to 80% [23]. Clearly, these hour-order charging time may not be acceptable when the user has only limited time to charge the battery.

• **Faster ≠ Necessary.** Fast charging is not always needed with the usually over-designed battery capacity, especially in view of the fact that most users are likely to charge their batteries in the night [5, 13]. Let us again take EV as an example. Statistics show that 80% of the users only drive ≤50 miles per day [24]. On the other side of the story, EV battery packs are commonly rated with mileages over 200 miles, e.g., 270 miles for Tesla S. This way, the EVs for most users are likely to "survive" the daily usage with a battery pack fully charged in the morning, and then charge them again in the night where Level-3 charge is not really needed. Moreover, fully charging the battery may not be needed during the day time — the capacity enough for day-time usage would suffice.

• **Faster ≠ Desirable.** Last but not the least, fast charging is not desirable for cells as it leads to faster capacity fading, thus shortening the lifetime of cells[2] and increasing the system operation cost.

Fast charging is for the *Charge-and-Go* scenario where the user wants her battery to be charged quickly and then get on her way. This application scenario does not allow cells to rest after charging and does accelerate their capacity fading.

We demonstrate this finding via measurements of two sets of Lithium-ion cells and the NEWARE battery tester (Fig. 3). Table 2 summarizes the cells details. In the first set of measurements, we charge/discharge the Set-I cells for 10 cycles with a charge/discharge current of ±500mA, respectively. The charging terminates when the cell voltage reaches 4.1V and the discharging terminates when the voltage decreases to 3.0V. A rest period of 0–60 minutes is inserted between each charge and discharge. Fig. 4(a) plots the averaged capacity fading of these cells during these 10 cycles, normalized to the delivered capacity in the first cycle. The cell capacity degrades slower with longer relaxation, e.g., to 98.2% of the first cycle when relaxing cells for 30 minutes after each charge, much slower than the case with no relax-

[1]The QC 3.0 released in Sep. 2015 is reported to take 35 minutes to charge the cell to 80% [21].

[2]It is a common practice to conclude a cell as died after its capacity fades to 80% of the rated level.

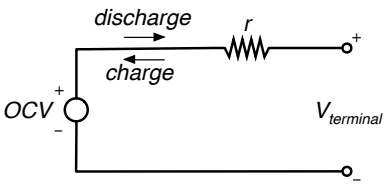

Figure 1: Circuit model of cells.

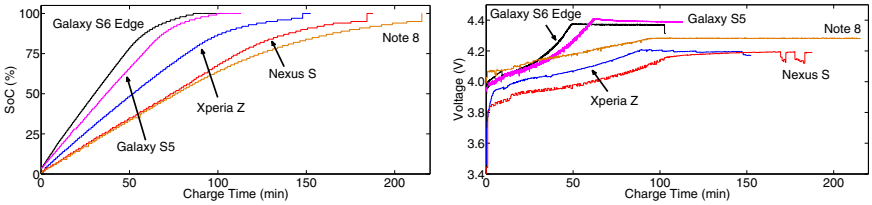

(a) SoC traces **(b)** Voltage traces

Figure 2: Charging processes of 5 mobile devices with respective chargers.

Figure 3: Battery tester and cells.

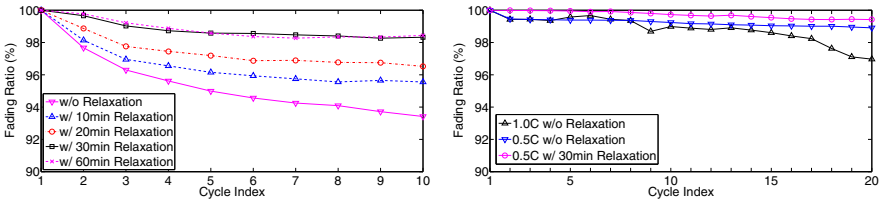

(a) Set-I cells over 10 cycles **(b)** Set-II cells over 20 cycles

Figure 4: Insufficient relaxation leads to accelerated cell capacity fading.

ation (i.e., 93.4%). However, an extremely long relaxation has diminishing effect on the slowdown of capacity fading, as observed from comparison of the cases with relaxation periods of 30 and 60 minutes.

Similar cycling tests have been performed with Set-II cells as shown in Fig. 4(b). Again, relaxing cells slows down their capacity fading. Also, comparison of the two cases with no relaxation reveals dramatic capacity fading when charging cells with higher current, reinforcing the necessity of relaxing cells after fast charging. Another observation is that relaxing cells to slow down their capacity fading is particularly crucial for aged cells, as revealed by comparison of Figs. 4(a) and (b). As the first investigation in this direction, we assume the needed relaxation time of cells, e.g., 30 minutes for Set-I cells as shown in Fig. 4(a), is provided by the cell manufacturer in the rest of this paper.

These three observations reveal that fast charging is not always the best to charge cells because (i) fast charging is agnostic of real-time user requirements, e.g., the available charging time, and thus blindly pushes for high current charging even if unnecessary; (ii) fast charging ignores the needed relaxation of cells, leading to accelerated capacity fading. So, we tackle the cell charging problem from a new perspective and aim to maximize the charged capacity within the user-specified available charging time $T_{\text{available}}$ while ensuring a relaxation period to be no shorter than T_{relax}, i.e.,

$$\begin{aligned} & \max \quad C_{\text{total}} \\ s.t. \quad & t_{\text{total}} \le T_{\text{available}} \quad \text{and} \quad t_{\text{relax}} \ge T_{\text{relax}}. \end{aligned} \tag{2}$$

4. CV-CHG SERVES AS RELAXATION

Resting cells (as in Fig. 4) is not desirable to maximize the charged capacity, albeit serving as relaxation. Here we show that the completed CV-Chg — the second phase of the classic CCCV charge — also serves as relaxation. We then introduce the challenges in relaxing cells via CV-Chg.

4.1 Why CV-Chg Serves as Relaxation?

Essentially, relaxation cools down the chemical reactions in the cells; otherwise, the oxidation of the electrolyte at the surface of cathode would form a resistive surface layer quickly [1, 14]. This also reduces the loss of active materials needed for the transformation between electrical and chemical energy. The essence of relaxation inspires us that gradually decreasing the charging current may also serve as relaxation for cells, as in the CV-Chg of CCCV charge.

CCCV is a classical charging method for Lithium-ion cells, widely implemented in both high/low-ends and small/large battery-powered systems [27,28]. Fig. 5 illustrates the CCCV-based charging process [25], which can be described by

$$< I_{\text{cc}}, \quad V_{\text{max}}, \quad I_{\text{cutoff}} >_{\text{cccv}}$$

and consists of the CC-Chg phase first and then the CV-Chg phase. In CC-Chg, the cell is charged with a large current I_{cc} (normally 0.5–1C) until its voltage reaches the maximum level V_{max}. Then, CV-Chg starts and charges the cell with voltage V_{max}, gradually decreasing charging current due to the increase of cell OCV. The CV-Chg completes when the charging current reduces to a pre-defined cut-off level I_{cutoff}, e.g., 0.05C [8, 14]. Both I_{cc} and I_{cutoff} are specified by the manufacturer for a particular model of cells, and V_{max} is normally in the range of 4.2–4.25V. The CCCV-based charging process can also be observed in Fig. 2.

The decreasing charging current makes CV-Chg serve as relaxation. To validate this, we charge the Set-I cells in Table 2 with <500mA, 4.2V, $I_{\text{cutoff}}>_{\text{cccv}}$ where $I_{\text{cutoff}} = \{150, 200, 300, 500\}$mA, and then discharge them with −500mA current until their voltages decrease to 3.0V. The case of $I_{\text{cutoff}} = 150$mA corresponds to the specified cutoff current of the cell, i.e., 0.05C, implying a *completed* CV-Chg. Specifically, we say a CV-Chg is *completed* if it terminates when the charging current decreases to the specified cutoff level. On the other hand, the cases with $I_{\text{cutoff}} = \{200, 300, 500\}$mA indicate pre-terminated CV-Chg. Note that there is actually no CV-Chg with $I_{\text{cutoff}} = 500$mA. Fig. 6(a) plots the averaged capacity fading over 10 such charge/discharge

Table 1: Level 1–3 charging for EVs.

	Charge Power	Charge Current	Charge Time	Infrastructure Cost
Level-1	1.4kW	15–20A	10 hour to fully charge	$230–1,350
Level-2	3.3kW	up to 80A	2–3 hour to fully charge	$2,600–21,000
Level-3	50kW	120–500A	30 minutes to 80%	$25,000–85,000

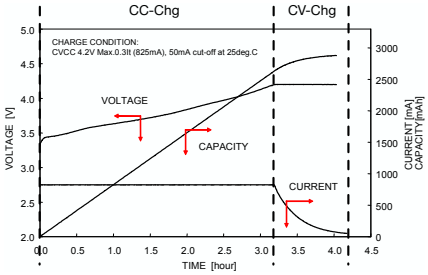

Figure 5: CCCV-based charging process [25].

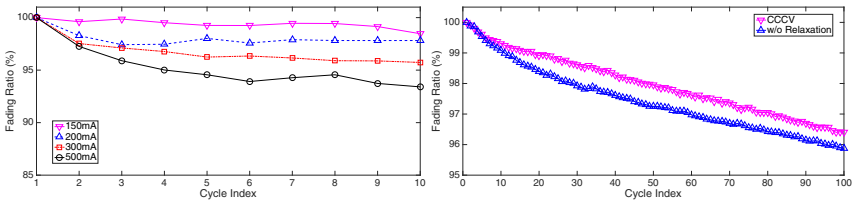

(a) Set-I cells over 10 cycles **(b)** Set-II cells over 100 cycles

Figure 6: Completed CV-Chg also serves as relaxation.

Table 2: Cells used in the measurements.

	Set-I	Set-II
Brand	UltraFire	TENERGY
Number of Cells	8	5
Rated Capacity	3,000mAh	2,600mAh
Age	2+ years	new

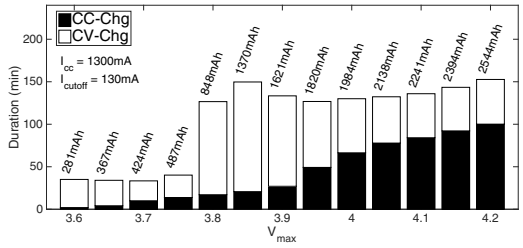

Figure 7: With CCCV, a smaller $V_{\max}$ leads to less charged capacity but not necessarily a shorter charging time.

cycles, showing that CV-Chg slows down the capacity fading of cells as it approaches completion, validating our conjecture that completed CV-Chg serves as relaxation. Similar cycling measurements have been performed with the Set-II cells and similar observations can be obtained (Fig. 6(b)).

4.2 Challenges in Relaxing via CV-Chg

Relaxing cells with CV-Chg is more promising than resting them as more capacity can be charged. However, the original CCCV is designed to fully charge cells, which is likely to be infeasible with limited $T_{\text{available}}$. A simple mitigation is to use a smaller (but as large as possible) voltage level $V'_{\max}$ to substitute $V_{\max}$ in $<I_{\text{cc}}, V_{\max}, I_{\text{cutoff}}>_{\text{cccv}}$, i.e., only partially charge the cell to ensure the charging process will complete within $T_{\text{available}}$. However, this approach may not work because charging less capacity to cells with CCCV does not necessarily lead to a shorter charging time. To demonstrate this, we use the modified CCCV to charge a cell with varying $V'_{\max}$. Fig. 7 compares the thus-collected charging durations and charged capacity — a smaller $V'_{\max}$ does lead to less charged capacity, but not necessarily a shorter charge time.

This finding needs to be reasoned with two aspects: the nonlinear relation between the OCV and depth-of-discharge (DoD)[3] of cells and the role $V_{\max}$ plays in CCCV.

• **Nonlinearity between OCV and DoD.** Lithium-ion cells demonstrate a monotonic relationship between their OCVs and DoDs as shown in Fig. 8(a). This relationship is stable for cells of the same chemistry and does not vary much with manufacturer (e.g., <5mV variances in OCV with given DoD [29]). Also, this relationship is available in the form of an OCV-DoD table in many off-the-shelf battery management chips, such as bq2750x from TI [30]. Fig. 8(b) plots our empirically obtained OCV-DoD curves with two cells, whose closeness validates the stable relationship. We will elaborate more on how these curves are obtained in Sec. 6. We use $\mathbb{D}(v)$ and $\mathbb{O}(d)$ to refer to the mapping between cell DoD and OCV in the rest of the paper.

Fig. 8 also shows that the OCV-DoD relation is not linear. Specifically, the OCVs are more sensitive to DoDs when cells are nearly fully charged (e.g., below 20% DoD) or completely discharged (e.g., approaching 100% DoD), but are not so sensitive in certain middle ranges, e.g., between 40–80% DoD.

• **Roles of $V_{\max}$ in CCCV.** $V_{\max}$ plays two roles in CCCV by answering two questions: when should CC-Chg terminate and how to charge during CV-Chg?

Specifically, we know the following details of CC-Chg and CV-Chg when using $<I_{\text{cc}}, V_{\max}, I_{\text{cutoff}}>_{\text{cccv}}$ to charge a cell with initial OCV v_0 (and an initial DoD $d_0 = \mathbb{D}(v_0)$) and internal resistance r.[4]

CC-Chg is responsible for charging the cell from OCV v_0 to $v_{\text{cc}} = V_{\max} - I_{\text{cc}} \cdot r$, and thus the capacity charged during CC-Chg is

$$C_{\text{cc}} = (\mathbb{D}(v_0) - \mathbb{D}(v_{\text{cc}})) \cdot C_0/100,$$

where C_0 is the total capacity of the cell upon being fully

[3]DoD describes the cell capacity that has been discharged as a percentage of its maximum capacity C_0.

[4]We assume a constant r during the charging process for the ease of description, which will be elaborated in Sec. 5.2.

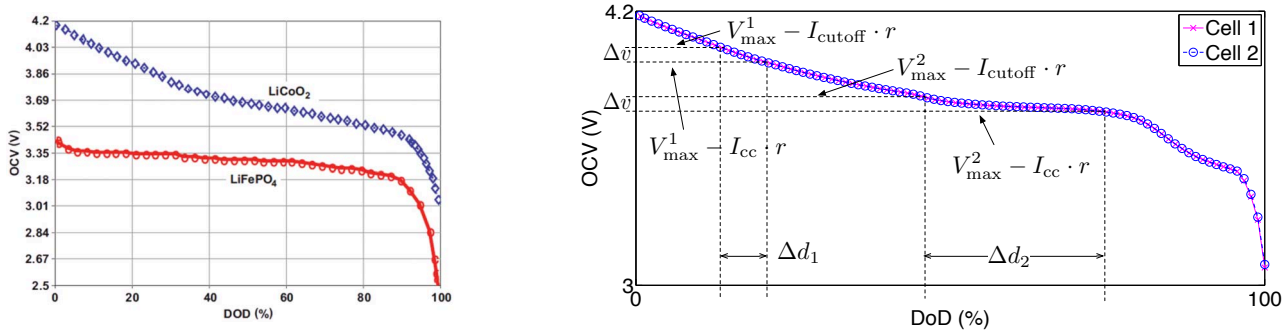

(a) Data reported by TI [26]

(b) Data collected via our measurements

Figure 8: The OCVs and DoDs of cells demonstrate reliable but nonlinear relationship.

charged. CC-Chg lasts for

$$T_{\text{cc}} = C_{\text{cc}}/I_{\text{cc}}.$$

After CC-Chg, CV-Chg is responsible for further charging the cell from OCV v_{cc} to $v_{\text{cv}} = V_{\max} - I_{\text{cutoff}} \cdot r$. The capacity charged during CV-Chg is

$$C_{\text{cv}} = (\mathbb{D}(v_{\text{cc}}) - \mathbb{D}(v_{\text{cv}})) \cdot C_0/100.$$

The time is discretized into unit slot δ_t. CV-Chg starts with a charging current of $I_1^{cv} = I_{\text{cc}}$. After the first time slot, the cell DoD decreases to

$$d_1^{cv} = \mathbb{D}(v_{\text{cc}}) - 100 \cdot \delta_t \cdot I_{\text{cc}}/C_0,$$

and its OCV rises to

$$v_1^{cv} = \mathbb{O}(d_1^{cv}).$$

This way, the charge current reduces to

$$I_2^{cv} = (V_{\max} - v_1^{cv})/r$$

during the second time slot. The process continues until the charging current decreases to I_{cutoff}. This way, CV-Chg duration T_{cv} can be calculated iteratively.

Now, let us consider the case when reducing $V_{\max}$ from $V^1_{\max}$ to $V^2_{\max}$ ($V^1_{\max} > V^2_{\max}$). The OCV range within which CC-Chg applies shrinks from $[v_0,\ V^1_{\max} - I_{\text{cc}} \cdot r]$ to $[v_0,\ V^2_{\max} - I_{\text{cc}} \cdot r]$, leading to less to-be-charged capacity and shorter CC-Chg duration. However, the OCV ranges to which the CV-Chg is responsible are

$$[V^1_{\max} - I_{\text{cc}} \cdot r,\quad V^1_{\max} - I_{\text{cutoff}} \cdot r],$$

and

$$[V^2_{\max} - I_{\text{cc}} \cdot r,\quad V^2_{\max} - I_{\text{cutoff}} \cdot r],$$

before and after the change, respectively. These OCV ranges may map to very different DoD intervals (and thus to-be-charged capacities) because of the nonlinear OCV-DoD table, although sharing the same OCV gap, i.e., $(I_{\text{cc}} - I_{\text{cutoff}}) \cdot r$. This is illustrated in Fig. 8(b) where the same magnitude of OCV change (i.e., Δv) leads to significantly different magnitudes of DoD changes (i.e., $\Delta d_1 << \Delta d_2$). Thus, reducing $V_{\max}$ shortens CC-Chg because of its first role, but may lead to longer CV-Chg with its second role (e.g., as in Fig. 7) — the overall charging time is not necessarily reduced.

To address this discrepancy between the charging time and charged capacity, in $*$-AWARE, we separate the two roles

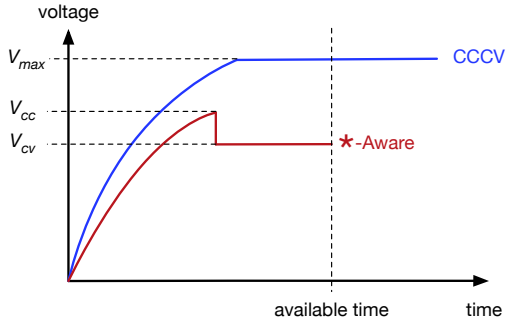

Figure 9: Illustration on the $*$-AWARE-based charging process.

```
for V_CV = 0, 1, ...., V_max
    for V_CC = 0, 1, ...., V_max
        identify < T_CC , C_CC > and < T_CV , C_CV >
    end
end
return the best combination of V_CV and V_CC
```

Figure 10: Basic principle of $*$-AWARE.

of $V_{\max}$ by introducing another control parameter as will be explained in the next section.

5. *-AWARE CHARGING

Besides the functional requirements on the charged capacity and charging time, simplicity is an important requirement for charging algorithms to facilitate their wide adoption. Here we first introduce the algorithm design of $*$-AWARE, demonstrating its computational simplicity, and then explain the simplicity of its implementation.

5.1 Basic Idea of $*$-AWARE

$*$-AWARE is an extended version of CCCV — a two-phase charging algorithm described by

$$< I_{\text{cc}},\quad V_{\text{cc}},\quad V_{\text{cv}},\quad I_{\text{cutoff}} >_{*\text{-AWARE}} \qquad (V_{\text{cc}} \geq V_{\text{cv}}).$$

Specifically, the $*$-AWARE-based charging process starts with CC-Chg with current I_{cc} until the cell voltage rises to V_{cc},

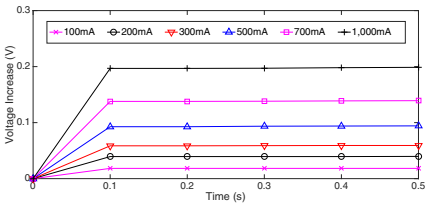

Figure 11: Voltage responses when charging a cell with different currents.

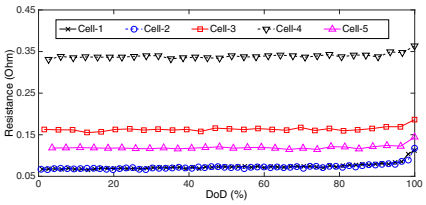

Figure 12: The cell resistance shows small variations throughout the charging process .

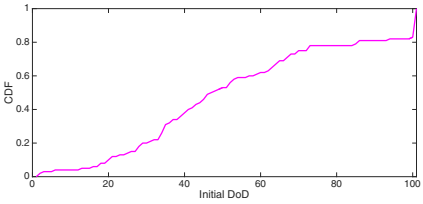

Figure 13: Mobile devices are often charged before completely discharged in most cases.

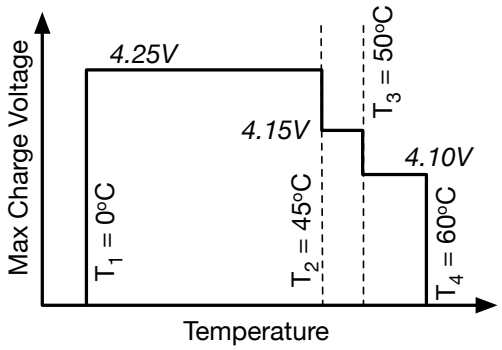

Figure 14: The maximum safe charge voltage of Lithium-ion cells with temperature [31].

and then CV-Chg charges the cell with voltage V_{cv} until the charging current falls to I_{cutoff}. This way, V_{cc} plays the first role of the original V_{max} in controlling CC-Chg and V_{cv} takes the second role of V_{max} in controlling CV-Chg. Fig. 9 illustrates the $*$-AWARE-based charging process and compares it with that of CCCV. The problem formulation in (2) can be refined as

$$\max \quad C_{\text{total}} = C_{\text{cc}} + C_{\text{cv}} \tag{3}$$

$$s.t. \quad T_{\text{cc}} + T_{\text{cv}} \leq T_{\text{available}} \tag{4}$$

$$T_{\text{cc}} \leq T_{\text{available}} - T_{\text{relax}}. \tag{5}$$

Thus, the basic principle of $*$-AWARE is to identify the optimal combination of V_{cc} and V_{cv}, as illustrated in Fig. 10.

Furthermore, we know

$$\max \quad C_{\text{total}} = C_{\text{cc}} + C_{\text{cv}} \quad \Leftrightarrow \quad \max \quad V_{\text{cv}}, \tag{6}$$

as V_{cv} determines the final OCV of the cell after charging, which is monotonic in the DoD of cells. Similarly, the constraint (5) can be transformed to

$$\begin{aligned} & T_{\text{cc}} \leq T_{\text{available}} - T_{\text{relax}} \\ \Leftrightarrow \quad & C_{\text{cc}} \leq C_{\text{cc,max}} = (T_{\text{available}} - T_{\text{relax}}) \cdot I_{\text{cc}} \\ \Leftrightarrow \quad & d_{\text{cc}} \geq d_{\text{cc,min}} = \max\{d_0 - \frac{C_{\text{cc,max}}}{C_0} \times 100\%,\ 0\} \\ \Leftrightarrow \quad & V_{\text{cc}} \leq \mathbb{O}(d_{\text{cc,min}}) + I_{\text{cc}} \cdot r. \end{aligned} \tag{7}$$

5.2 Prediction with Given V_{cc} and V_{cv}

The first component in $*$-AWARE is to predict (i.e., determine T_{cc}, C_{cc}, T_{cv}, and C_{cv}) the charging process with given V_{cc} and V_{cv}. The basic prediction principle is based on the OCV-DoD table as described in Sec. 4.2, for which the cell resistance r is needed.

$*$-AWARE estimates the cell resistance based on the basic physics $r = V/I$. Specifically, $*$-AWARE inputs short current pulses to the cell and records its voltage responses before actually charging it. This way, the cell resistance can be estimated by $r = \Delta V/I$, where ΔV is the increase of cell voltage and I is the input current. Fig. 11 shows the voltage responses of a cell with different current pulses — the voltage increases quickly during the first 0.1s because of the $I \cdot r$ voltage and then increases slowly due to the charging of the cell. The quick response of the $I \cdot r$ voltage allows $*$-AWARE to estimate r with little overhead, e.g., r=0.19Ω for the cell in Fig. 11. $*$-AWARE uses the thus-estimated r to predict the charging process with given V_{cc} and V_{cv}.

However, cell resistance is known to be variable during charging. To gain more insight on this, we intermittently charge 5 cells to estimate their r in real time throughout the charging process — charging the cells with constant current for 10s and then stop the current for 10s, repeat the process until the cell voltage reaches 4.2V. Fig. 12 plots the thus-collected resistance traces, which are indeed not constant. However, the variations of cell resistance is small except when the cells are of extreme high DoDs, or when they are nearly completely discharged.

For battery-powered systems such as mobile devices and EVs, users typically charge the system before completely draining its battery. We have collected a usage trace of a Galaxy S6 Edge for 29 days. Fig. 13 plots the distribution of battery DoDs when the charging of the phone begins during the recorded periods — the phone is charged before its battery reaches 80% DoD in more than 80% of all the cases. Similar observation is reported in [32]. For EVs, the studies in [33, 34] show EVs are normally charged before their batteries reach 70% DoD. These observations indicate that charging cells with extreme high initial DoDs is not common in practice. Thus, it is reasonable for $*$-AWARE to predict the charging process with the before-charge-r, the accuracy will later be validated empirically in Sec. 6.

5.3 Identifying the Optimal V_{cc} and V_{cv}

Knowing how to predict the charging process with given V_{cc} and V_{cv}, we need to find an optimal combination of the two. $*$-AWARE identifies the optimal combination by first reducing the search space and then guiding the search therein.

• **Reducing the Search Space.** The search space for V_{cc} and V_{cv} can be reduced as follows. First, there are constraints on the maximum voltage to charge cells safely, i.e., $V_{\text{safe,max}}$, as specified by JEITA and as shown in Fig. 14 [31].

Second, a voltage higher than the cell OCV is required to charge the cell. At the beginning of the charging process, this means that the charging voltage has to be higher than the cell's initial OCV v_0. This lower bound of the charging

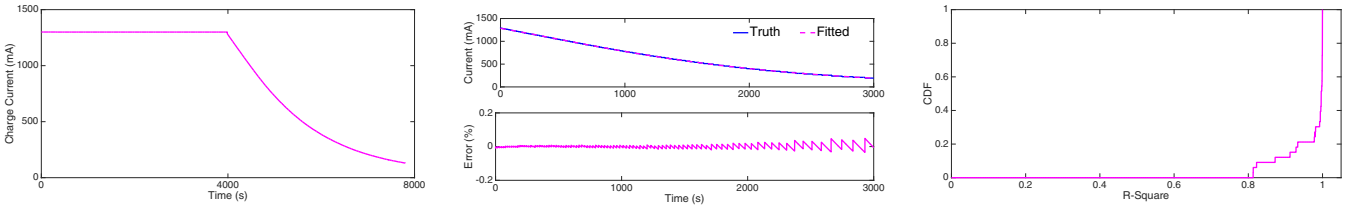

(a) Current curve **(b)** Fitting as exponential and fitting error **(c)** Goodness-of-fit distribution

Figure 15: The charging current during CV-Chg fits a two-term exponential model.

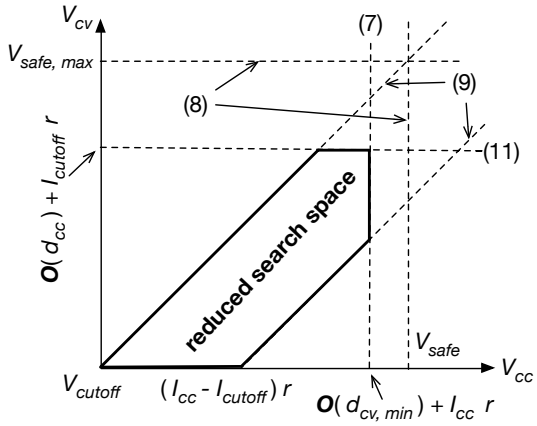

Figure 16: Reduced search space.

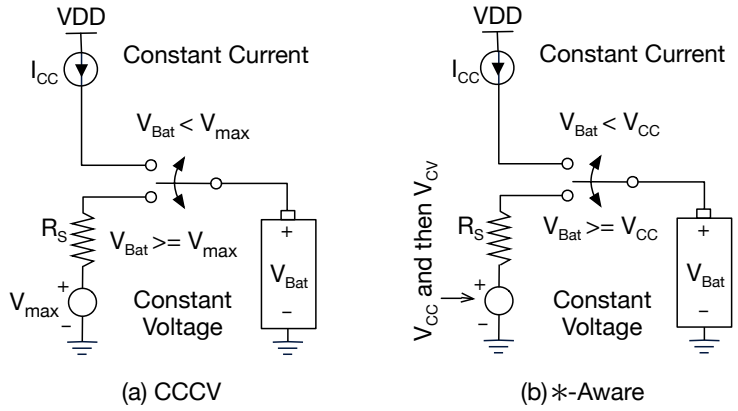

Figure 17: Implementation circuit schemata for CCCV and ∗-AWARE.

voltage is tightened further to $(v_0+I_{\rm cc}\cdot r)$ to achieve the CC-Chg current $I_{\rm cc}$. Combining with the maximum safe charge voltage, we know

$$v_0 + I_{\rm cc}\cdot r \le V_{\rm cv} \le V_{\rm cc} \le V_{\rm safe,max}. \tag{8}$$

Furthermore, when switching from CC-Chg to CV-Chg, this observation requires

$$V_{\rm cv} - (V_{\rm cc} - I_{\rm cc}\cdot r) \ge I_{\rm cutoff}\cdot r\ ;$$

otherwise, there will be no CV-Chg. After making some arrangements, we get

$$V_{\rm cc} - (I_{\rm cc} - I_{\rm cutoff})\cdot r \le V_{\rm cv} \le V_{\rm cc}. \tag{9}$$

Last but not the least, we have another upper bound of $V_{\rm cv}$ by observing the CV-Chg current trace is convex. Fig. 15(a) plots the current when charging a cell with <1, 300mA, 4.1V, 130mA>$_{\rm cccv}$. The CV-Chg current conforms to a two-term exponential decay process $I_t^{\rm cv} = ae^{b\cdot t} + ce^{d\cdot t}$ for certain a, b, c, and d. Fig. 15(b) plots the corresponding exponentially-fitted curve, demonstrating high fitting accuracy, i.e., with error ≤0.15%. To further validate this hypothesis, we apply the two-term exponential fit to 33 empirically collected CV-Chg current traces, and the thus-collected distribution of the goodness-of-fit (in R-Squared) is shown in Fig. 15(c). All of these fittings have R-Squared larger than 0.8, and over 70% of them have a R-Squared ≥0.99. These statistics on fitting goodness indicate a good match between the current traces and the fitted curves, validating our hypothesis that the charging current during CV-Chg conforms to a two-term exponential decay process.

Exponential functions are convex, hence showing that the CV-Chg current trace $\{I_1^{\rm cv},\ I_2^{\rm cv},\ \cdots,\ I_{T_{\rm cv}}^{\rm cv}\}$ is also convex (note that $I_{T_{\rm cv}}^{\rm cv} = I_{\rm cutoff}$). This way, we know for any $t \in [1, T_{\rm cv}]$

$$I_t^{\rm cv} \le \frac{T_{\rm cv}-t}{T_{\rm cv}} I_1^{\rm cv} + \frac{t}{T_{\rm cv}} I_{T_{\rm cv}}^{\rm cv},$$

based on which we have the following upper bound on the capacity charged during CV-Chg:

$$C_{\rm cv} = \int_0^{T_{\rm cv}} I_t^{\rm cv}\,dt \le \frac{(I_{\rm cc}+I_{\rm cutoff})\cdot T_{\rm cv}}{2}. \tag{10}$$

This in turn leads to the following upper bound on the total capacity charged with ∗-AWARE:

$$\begin{aligned} C_{\rm total} &= C_{\rm cc} + C_{\rm cv} \\ &\le I_{\rm cc}\cdot T_{\rm cc} + \frac{(I_{\rm cc}+I_{\rm cutoff})\cdot T_{\rm cv}}{2} \\ &\le I_{\rm cc}\cdot T_{\rm cc} + \frac{(I_{\rm cc}+I_{\rm cutoff})\cdot (T_{\rm available}-T_{\rm cc})}{2} \\ &\le \frac{(2\cdot T_{\rm available} - T_{\rm relax})\cdot I_{\rm cc} + T_{\rm relax}\cdot I_{\rm cutoff}}{2} = C_{\rm max}. \end{aligned}$$

Thus, we have the lower bound of the cell's DoD after charging it as

$$d_{\rm min} > \max\{d_0 - \frac{100\cdot C_{\rm max}}{C_0}, 0\}.$$

Mapping DoD to OCV, we get

$$V_{\rm cv} \le \mathbb{O}(d_{\rm min}) + I_{\rm cutoff}\cdot r. \tag{11}$$

The above three facts help further refine the problem formulation in (3) as

$$\begin{aligned} &\max \quad V_{\rm cv} \\ &s.t. \quad (4), (7), (8), (9), (11). \end{aligned} \tag{12}$$

• **Searching in the Reduced Space.** Fig. 16 illustrates an example of reduced search space by jointly considering constraints (7), (8), (9), and (11), which can be easily identified for any given problem instance. The last step is to find the optimal solution in the reduced search space satisfying (4).

It is intuitive to search the space *top-down* as we aim to find the largest possible V_{cv}. Furthermore, only the rightmost (i.e., largest) V_{cc} needs to be considered when multiple points with the same V_{cv} exist in the search space, because the required charging time T_{total} monotonically decreases as V_{cc} increases with given V_{cv}. This observation is straightforward as V_{cv} determines the total capacity to be charged, and V_{cc} further determines how much capacity is charged with CC-Chg and CV-Chg, respectively. A larger V_{cc} indicates that more capacity are charged with CC-Chg, increasing the overall charge rate and reducing T_{total}. This guided search identifies the optimal[5] V_{cc} and V_{cv} based on the physical facts when charging cells, although it is greedy in nature.

5.4 Summary of ∗-Aware

Alg. 1 summarizes the workflow of ∗-Aware. The first step is to estimate the cell resistance r (line 2), with which the reduced search space can be identified (line 3). The guided search is then performed to find the optimal V_{cc} and V_{cv} (lines 6–14). The overall complexity of ∗-Aware is $\mathcal{O}(\frac{T_{\text{available}}}{\delta_t} lg \frac{1}{\delta_v})$, where the first term accounts for the complexity in predicting the charging process with given V_{cc} and V_{cv}, and the second term accounts for the complexity in looking up the OCV-DoD table with an OCV granularity of δ_v.[6]

5.5 Implementation Simplicity

Besides the low computational complexity, ∗-Aware is also simple to implement because its control principle is similar to CCCV, which has been widely deployed in both high- and low-end systems [7]. Fig. 17(a) shows the circuit diagram that implements CCCV, where the current source outputs I_{cc} and the voltage source supplies $V_{\max}$. The switch position controls whether CC-Chg or CV-Chg should be operational, which is determined based on real-time feedback of cell voltage. On top of this CCCV implementation, ∗-Aware poses only one additional requirement for the voltage source to supply V_{cc} first and then V_{cv} — an evolution from one single voltage threshold to two voltage thresholds sequentially, and all other circuit logic remains the same. The circuit schema for ∗-Aware is shown in Fig. 17(b).

6. EXPERIMENTS

We have experimentally evaluated ∗-Aware. Specifically, we first verify the accuracy of ∗-Aware in predicting the charging process and then evaluate its performance with respect to both the charged capacity and the capacity fading.

[5]With given search granularities and regarding to (12).

[6]The complexity for $\mathbb{D}(v)$ and $\mathbb{O}(d)$ are $\mathcal{O}(1)$ and $\mathcal{O}(lg \frac{V_{\max}}{\delta_v})$, respectively, assuming the table is constructed with OCV as indexes.

Algorithm 1 Pseudocode of ∗-Aware .

```
1: V_cc = −1, V_cv = −1;
2: Estimate resistance r;
3: Identify the reduced search space Z based on (7), (8), (9), and (11);
4: Find V_cv,min and V_cv,max in Z;
5: V_cv,tmp = V_cv,max;
6: while V_cv,tmp ≥ V_cv,min do
7:    Find the largest V_cc,tmp in Z with V_cv,tmp;
8:    Predict the charging process with <I_cc, V_cc,tmp, V_cv,tmp, I_cutoff>_∗-Aware;
9:    if T_cc + T_cv ≤ T_available then
10:      V_cc = V_cc,tmp, V_cv = V_cv,tmp;
11:      break;
12:   else
13:      V_cv = V_cv − δ_v;
14:   end if
15: end while
16: return V_cc and V_cv;
```

6.1 Collecting the OCV-DoD Table

TENERGY ICR 18650-2600 Lithium-ion cells are used for our experiments; its OCV-DoD table is required for ∗-Aware to predict the charging process. To obtain this OCV-DoD table, we use the battery tester to charge the cells with 200mA current and record the process, based on which we can identify the relationship between the terminal voltage and DoD of the cells. We then perform resistance compensation on the thus-collected traces based on Eq. (1) to derive the OCV-DoD table. The small charging current (i.e., 200mA or $200/2600 \approx 0.077$C) is to reduce the $I \cdot r$ voltage and thus improve the accuracy of the derived OCD-DoD table. The OCV-DoD curves we obtained are plotted in Fig. 8(b).

6.2 Prediction Accuracy

We verify the accuracy of ∗-Aware in predicting the charging process based on the OCV-DoD table. Specifically, we collect 34 charging traces of cells with different voltages and currents, serving as the ground truth. We then use ∗-Aware to predict these charging processes with their corresponding voltages and currents based on the OCV-DoD table. Fig. 18 summarizes the predication accuracy, where the x-axis is the error in predicted charging time and the y-axis is the error in predicted charged capacity. The prediction is found to be pretty accurate — the error in predicting the charged capacity is in the range of $[-1.33\%, 5.44\%]$ with an average of 0.74%, and that in predicting the charging time is $[-7.82\%, 5.33\%]$ with an average of -2.26%.

6.3 Charged Capacity

Next, we evaluate the charged capacity with ∗-Aware and compare it with the following two baselines both of which also ensure enough relaxation.

- **Greedy Fast (G-Fast).** With G-Fast, the cells are greedily charged with I_{cc} for a time period of $(T_{\text{available}} - T_{\text{relax}})$ — charge cells with the large current I_{cc} as long as possible.

- **Modified CCCV (M-CCCV).** Similar to the original CCCV, M-CCCV is described by a triple $<I_{\text{cc}}$,

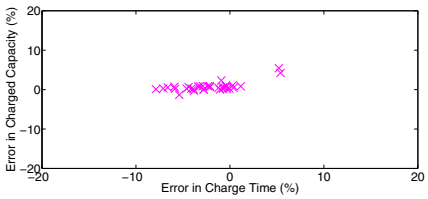

Figure 18: Prediction accuracy.

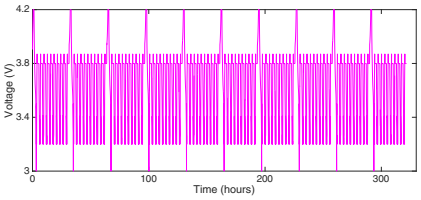

Figure 19: ∗-AWARE-based cycling test.

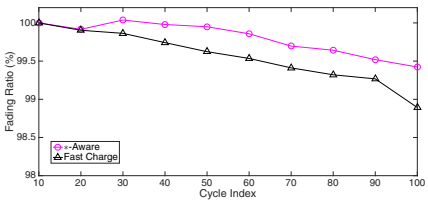

Figure 20: Capacity fading.

Table 3: Case study details.

	$T_{\text{available}}$	T_{relax}	Initial OCV	Profile w/ ∗-Aware	Profile w/ M-CCCV	Profile w/ G-Fast
Case-I	60min	30min	3.20V	$<1,300,3.9152,3.7930,130>$	$<1,300,3.7788,130>$	1,300mA for 30min
Case-II	60min	30min	3.75V	$<1,300,4.0101,3.8811,130>$	$<1,300,3.8002,130>$	1,300mA for 30min
Case-III	60min	40min	3.32V	$<1,300,3.9350,3.7989,130>$	$<1,300,3.7900,130>$	1,300mA for 20min
Case-IV	60min	40min	3.45V	$<1,300,3.9000,3.7887,130>$	$<1,300,3.7800,130>$	1,300mA for 20min
Case-V	60min	40min	3.57V	$<1,300,3.9701,3.8082,130>$	$<1,300,3.8000,130>$	1,300mA for 20min
Case-VI	60min	40min	3.71V	$<1,300,3.9601,3.8144,130>$	$<1,300,3.7950,130>$	1,300mA for 20min

$V'_{\max}, I_{\text{cutoff}}>_{\text{m-cccv}}$. However, M-CCCV identifies the optimal $V'_{\max}$ to maximize the charged capacity while ensuring enough relaxation, instead of using the fully charge voltage $V_{\max}$.

We conducted 6 case studies in which cells with different initial OCVs are charged with the three methods. The charging currents are $I_{\text{cc}} = 1,300$mA and $I_{\text{cutoff}} = 130$mA as specified by the cell manufacturer. The details of these case studies are listed in Table 3. Again, the battery tester is used to charge the cells according to these listed profiles.

Table 4 summarizes the charged capacity in these case studies.[7] ∗-AWARE outperforms the two baselines by 6.9–50.5%, and improvement ratios of 160% and 290% are observed in Case-II and Case-VI over M-CCCV. This almost 3x improvement over M-CCCV is achieved because in Case-II, the initial OCV (i.e., 3.74V) falls in the range where the DoDs are highly sensitive to OCVs. Recall that in M-CCCV, CV-Chg is responsible to charge the cell in the OCV range $[V_{\max} - I_{\text{cc}} \cdot r, V_{\max} - I_{\text{cutoff}} \cdot r]$, which corresponds to a wide range of DoDs in Case-II. This means that the CV-Chg is responsible for charging more capacity to cells and thus requiring more time. As a result, the CC-Chg phase is short and the overall charged capacity is limited. These results further reinforce the necessity to separate the control over CC-Chg and CV-Chg, as in ∗-AWARE.

6.4 Capacity Fading

We also evaluate the effect of ∗-AWARE in slowing down the capacity fading of cells with cycles. Specifically, we repeat Case-I in Table 3 for 100 cycles with ∗-AWARE and fast charging, respectively.[8] We fully charge and discharge the cells every 10 cycles to collect their total deliverable capacities. 6 cells are used in these cycling tests, and Fig. 19 shows an exemplary voltage trace when cycling with ∗-AWARE. Fig. 20 plots the averaged capacity fading during these cycling tests. The cell capacity fades to 99.44% with ∗-AWARE and to 98.89% when fast charging is used.

Moreover, 92,884.0mAh capacity is delivered on average during the ∗-AWARE-based cycling tests, and that with fast charging is 140,835.0mAh. Normalizing the delivered capacity with the capacity fading ratios, we find that the cell capacity degrades 1% after delivering 165,860mAh capacity when cycling with ∗-AWARE, while that with fast charging is only 127,150mAh.

These two comparisons show that ∗-AWARE not only slows down the capacity fading of the cells by $1-\frac{1-0.9944}{1-0.9889} = 49.55\%$, but more importantly, also increases the total capacity the cells deliver during their lifetime by $\frac{165,860-127,150}{127,150} = 30.45\%$.

7. RELATED WORK

Charging Lithium-ion cells is a complex electrochemical process. Zhang *et al.* [1] explored how the charge current and ambient temperature change the anode and cathode during charging. The effect of various charge protocols on the cycle life of cells was investigated in [14].

These studies of the charging process facilitate the design of fast charge technologies, to which significant effort has been devoted at different layers of abstraction, including algorithms [8–11], circuit topology [7], and specially-designed cells [6]. For example, Boostcharging [8] pushes for large current charging by directly charging drained batteries in the CV mode. A variable frequency pulse charging system was proposed in [10] and a fuzzy-controlled charging design was presented in [9]. Chen *et al.* [11] developed a charging algorithm based on grey predication. A circuit topology for battery charging was proposed in [7], demonstrating the advantage of phase-locked loop. A unique type of Lithium-ion cell that can be charged in a few minutes was proposed in [6].

However, two important factors have been overlooked in these designs: the available charge time for the user and the desired after-charge relaxation for cells. ∗-AWARE accounts for these factors and completes the charging paradigm when fast charging of cells is not needed. The model-based simulation has shown that relaxation after discharge helps improve the cycle life of Lithium-ion cells [15], complementing our empirical finding on the after-charge relaxation.

8. CONCLUSIONS

Pursuing fast charge is not always needed and accelerates the capacity fading of cells due to its inability to rest

[7]Actually, the charged capacity with G-Fast can be calculated directly using given I_{cc}, $T_{\text{available}}$, and T_{relax}, e.g., $1,300 \times (3,600 - 1,800)/3,600 = 650$mAh in Case-I. The small variation in the experimental result (i.e., 650.3mAh vs. 650mAh) is due to the accuracy of the battery tester in controlling the current (i.e., ±0.1mA).

[8]The cells are charged with 1,300mA current for 1 hour and then discharged to 3.20V in each of the cycles with fast charging.

Table 4: Experiment results on charged capacity.

	Charged Capacity (mAh)			Improvement Ratio (%)	
	∗-Aware	M-CCCV	G-Fast	over M-CCCV	over G-Fast
Case-I	703.3	589.3	650.4	19.3	8.1
Case-II	743.6	188.8	650.3	293.9	14.4
Case-III	578.0	521.6	433.6	10.8	33.3
Case-IV	567.9	531.3	433.0	6.9	31.2
Case-V	533.8	354.8	433.5	50.5	23.1
Case-VI	562.2	215.4	433.3	161	29.7

cells after charge. In this paper, we have tackled the cell charging problem from a new perspective. Specifically, we have proposed ∗-Aware, a {user, cell}-aware charging algorithm that maximizes the charged capacity within the user-specified available charge time while ensuring enough relaxation for cells to slow down their capacity fading. Extensive experiments and trace-driven emulations have shown that ∗-Aware increases the charged capacity by 6.9–50.5% and up to 3x in certain extreme cases, and slows down the capacity fading of cells by 49.55%.

Acknowledgment: The work reported in this paper was supported in part by NSF under Grants CNS-1329702 and CNS-1446117.

9. REFERENCES

[1] S. Zhang, K. Xu, and T. Jow, "Study of the charging process of a $LiCoO_2$-based Li-ion battery," *Journal of Power Sources*, vol. 160, pp. 1349–1354, 2006.

[2] K. Vatanparvar and M. A. A. Faruque, "Battery lifetime-aware automotive climate control for electric vehicles," in *DAC'15*, 2015.

[3] L. He, Y. Gu, C. Liu, T. Zhu, and K. G. Shin, "SHARE: SoH-aware reconfiguration to enhance deliverable capacity of large-scale battery packs," in *ICCPS'15*, 2015.

[4] "Tesla Model S," http://www.roperld.com/science/TeslaModelS.htm.

[5] C. Botsford and A. Szczepanek, "Fast charging vs. slow charging: Pros and cons for the new age of electric vehicles," in *EVS24*, 2009.

[6] K. Zaghib, M. Dontigny, A. Guerfi, P. Charest, I. Rodrigues, A. Mauger, and C. Julien, "Safe and fast-charging Li-ion battery with long shelf life for power applications," *Journal of Power Sources*, vol. 196, pp. 3949–3954, 2011.

[7] L.-R. Chen, "PLL-based battery charge circuit topology," *Journal of Power Sources*, vol. 51, no. 6, pp. 1344–1346, 2004.

[8] P. Notten, J. O. het Veld, and J. van Beek, "Boostcharging Li-ion batteries: A challenging new charging concept," *Journal of Power Sources*, vol. 145, pp. 89–94, 2005.

[9] G.-C. Hsieh, L.-R. Chen, and K.-S. Huang, "Fuzzy-controlled Li-ion battery charge system with active state-of-charge controller," *IEEE Transactions on Industrial Electronics*, vol. 48, no. 3, pp. 585–593, 2001.

[10] L.-R. Chen, "A design of an optimal battery pulse charge system by frequency-varied technique," *IEEE Transactions on Industrial Electronics*, vol. 54, no. 1, pp. 398–405, 2007.

[11] L.-R. Chen, R. C. Hsu, and C.-S. Liu, "A design of a grey-predicted Li-ion battery charge system," *IEEE Transactions on Industrial Electronics*, vol. 55, no. 10, pp. 3692–3701, 2008.

[12] W. A. van Schalkwijk and R. S. Penn, "Lithium-ion rapid charging system and method," *US patent, 7,227,336 B1*, 2007.

[13] M. Y. Arslan, I. Singh, S. Singh, H. V. Madhyastha, K. Sundaresan, and S. V. Krishnamurthy, "Computing while charging: Building a distributed computing infrastructure using smartphones," in *CoNEXT'12*, 2012.

[14] S. S. Zhang, "The effect of the charging protocol on the cycle life of a Li-ion battery," *Journal of Power Sources*, vol. 161, pp. 1385–1391, 2006.

[15] M. Rashid and A. Gupta, "Effect of relaxation periods over cycling performance of a Li-ion battery," *Journal of The Electrochemical Society*, vol. 162, no. 2, pp. A3145–A3153, 2015.

[16] "Nissan LEAF Warranty," http://www.nissanusa.com/electric-cars/leaf/charging-range/battery/.

[17] D. Andrea, "Battery management systems for large Lithium-ion battery packs," *Artech House*, 2010.

[18] G. Ning and B. N. Popov, "Cycle Life Modeling of Lithium-ion Batteries," *Journal of The Electrochemical Society*, vol. 151, no. 10, pp. A1584–A1591, 2004.

[19] L. He, L. Gu, L. Kong, Y. Gu, C. Liu, and T. He, "Exploring adaptive reconfiguration to optimize energy efficiency in large-scale battery systems," in *RTSS'13*, 2013.

[20] L. He, S. Ying, and Y. Gu, "Demo: Reconfiguration-based energy optimization in battery systems: a testbed prototype," in *RTSSWork'13*, 2013.

[21] "QC 3.0," http://www.droid-life.com/2015/09/14/qualcomm-quick-charge-3-0/.

[22] "Range Anxiety," http://www.latimes.com/business/autos/la-fi-hy-tesla-story-so-far-20150318-htmlstory.html.

[23] "Field Trial: Level 3 Quick-Charging Two EVs," http://www.roperld.com/science/TeslaModelS.htm.

[24] "NHTS2009," http://nhts.ornl.gov/2009/pub/stt.pdf.

[25] "Panasonic NCR18650 Li-ion Battery," http://industrial.panasonic.com/www-data/pdf2/ACA4000/ACA4000CE240.pdf.

[26] "Battery Fuel Gauges Provide Accurate Range Prediction for eBikes, Light EVs," http://www.digikey.com/en/articles/techzone/2011/oct/battery-fuel-gauges-provide-accurate-range-prediction-for-ebikes-light-evs.

[27] L. He, L. Kong, S. Lin, S. Ying, Y. Gu, T. He, and C. Liu, "Reconfiguration-assisted charging in large-scale Lithium-ion battery systems," in *ICCPS'14*, 2014.

[28] ——, "RAC: Reconfiguration-Assisted Charging in Large-Scale Lithium-Ion Battery Systems," *Smart Grid, IEEE Transactions on*, vol. PP, no. 99, pp. 1–1, 2015.

[29] "Battery Monitoring Basics," https://training.ti.com/sites/default/files/BatteryMonitoringBasics.ppt.

[30] M. Y. Y. Barsukov and M. Vega, "Theory and implementation of Impedance Track battery fuel-gauging algorithm in bq2750x family," *Application Report, SLUA450*, 2008.

[31] J. Qian, "Li-ion battery-charger solutions for JEITA compliance," *Analog Applications Journal*, pp. 8–11, 2010.

[32] D. Ferreira, A. K. Dey, and V. Kostakos, "Understanding human smartphone concerns: A study of battery life," in *Pervasive'11*.

[33] "The Smart Move Case Studies," http://www.cenex.co.uk/wp-content/uploads/2013/06/2011-11-21-Smart-Move-Case-Studies.pdf.

[34] T. Franke and J. F. Krems, "Understanding charging behavior of electric vehicle users," *Transportation Research Part F*, vol. 21, pp. 75–89, 2013.